ISSN 0023-1584, Kinetics and Catalysis, 2009, Vol. 50, No. 5, pp. 760–767. © Pleiades Publishing, Ltd., 2009.
Original Russian Text © G.A. Zenkovets, V.Yu. Gavrilov, A.A. Shutilov, S.V. Tsybulya, 2009, published in Kinetika i Kataliz, 2009, Vol. 50, No. 5, pp. 790–797.

Effect of Silicon Dioxide on the Formation of the Phase Composition and Pore Structure of Titanium Dioxide with the Anatase Structure

G. A. Zenkovets, V. Yu. Gavrilov, A. A. Shutilov, and S. V. Tsybulya

Boreskov Institute of Catalysis, Siberian Branch, Russian Academy of Sciences, Novosibirsk, 630090 Russia

e-mail: zenk@catalysis.ru

Received May 8, 2008

Abstract—The formation of the structure of titanium dioxide modified with silicon dioxide, which was introduced as tetraethyl orthosilicate, was studied. It was found that the formation of the nanocrystalline structure of TiO_2 occurred upon the modification of titanium dioxide with silicon dioxide. This nanocrystalline structure of TiO_2 was formed by highly dispersed anatase particles of size 6–10 nm stabilized by silicon oxide layers, which were formed upon the decomposition of tetraethyl orthosilicate. An increase in the modifier concentration resulted in a deceleration of the growth of anatase particles and an increase in the temperature of the phase transition of anatase to rutile. It was found that the anatase phase in the samples containing 5–15 wt % SiO_2 was stable up to 1000°C. The stabilization of highly dispersed anatase particles facilitated the retention of the developed fine-pore structure of xerogels with a pore diameter of 4 nm up to 900°C.

DOI: 10.1134/S002315840905019X

INTRODUCTION

Titanium dioxide with the anatase structure is widely used in various chemical technologies. It is used as a catalyst for various processes including the photocatalytic oxidation of organic impurities in air and water [1, 2] and as a support for heterogeneous catalysts including catalysts for protecting the environment from nitrogen oxides and carbon oxides [3, 4]. It is a highly efficient material for solar energy conversion into electric energy [5], for the manufacture of lithium cell electrodes [6], etc.

At the same time, the anatase modification of titanium dioxide is metastable and turns into rutile as the temperature is increased above 600–800°C. The phase transformation of anatase into rutile results in a dramatic decrease in the dispersity of particles and a change in their pore structure to impair the properties of the material as a support and a catalyst. For example, Vedrine [3] found that the phase transformation of anatase into rutile in supported V_2O_5/TiO_2 catalysts, which are commonly used in the protection of the environment from nitrogen oxides, resulted in a dramatic decrease in the activity of the catalyst.

It was noted that the procedure used in the preparation of TiO_2, including its modification by the addition of various metal cations, has a considerable effect on the thermal stability of anatase and on the temperature of the phase transition to rutile. For example, the additives of vanadium [7, 8], nickel [9], neodymium, and gadolinium [10, 11] considerably decreased the temperature of the phase transition of anatase to rutile, whereas the additives of chromium and tungsten [10, 12], as well as cerium [13] and silicon [14] increased this temperature.

There is no general agreement among authors as to the nature of the effect of modifying additives on the temperature of the phase transition of anatase to rutile. The decrease in the phase transition temperature was explained by the similarity between the crystal structures of the modifier and rutile facilitating the formation of substitutional solid solutions [12, 15, 16], by the formation of compounds with different bond strengths [11, 17], or by the decrease in the energy of formation of rutile nuclei at the anatase crystal–impurity crystal interface [16, 18].

In recent studies, including those performed on TiO_2 films supported onto various substrates, it was found that the initial anatase particle size and morphology are important factors affecting the temperature of the phase transition of anatase to rutile. Thus, Gribb and Banfield [19] were the first to demonstrate that, in nanosized titanium dioxide, anatase particles should reach a sufficiently large size in the course of thermal treatment in order for the phase transition to occur. Anatase is never transformed into rutile until the particle size increases to a certain critical value, for example, as a result of agglomeration. As found by calculations, as the particle size of TiO_2 is decreased, the free energy of the rutile modification increases considerably to exceed the corresponding values for anatase. As a result, the anatase phase becomes more stable for titanium dioxide with particles smaller than 14 nm;

because of this, the traditional phase transition is considerably hindered. As the particle size of TiO_2 is increased above the critical value of 14 nm, the system returns to its usual state when the rutile modification is thermodynamically more preferable. This statement was subsequently supported in other studies [20–26], although the estimated critical particle sizes of anatase were somewhat different in some cases. Thus, according to Fu et al. [25], this size was about 20 nm, whereas Zenkovets et al. [27] detected the occurrence of an anatase phase in titanium dioxide prepared using the industrial sulfuric acid technology to a particle size of 40 nm at 650°C.

It was found [28, 29] that, in TiO_2–SiO_2 mixed oxides at sufficiently high silicon contents, titanium silicalite with the MFI zeolite structure or anatase with a higher specific surface area, a high thermal stability, and a higher phase-transition temperature can be obtained. This higher phase-transition temperature was associated with the stabilization of highly dispersed anatase particles in the structure of amorphous silica gel and the formation of Ti–O–Si heterobonds. In addition, note that methods for the synthesis of TiO_2–SiO_2 mixed oxides, which consist in the hydrolysis or precipitation from organometallic compounds (or inorganic salts) of titanium and tetraethyl orthosilicate, are labor-intensive, energy-consuming, and associated with the formation of harmful wastes.

At the same time, there are almost no published data concerning the effect of the modification of titanium dioxide with silicon additives on the formation of its microstructure and pore structure and on its thermal stability at elevated temperatures. Although the effects of various additives on the temperature of the phase transition of anatase to rutile have been intensively studied, the reasons for this phenomenon remain unclear. To clarify this problem, the effects of modifying additives on the bulk and surface microstructures of TiO_2 should be studied. Recently, these studies became possible with the appearance of precision investigation techniques, including high-resolution electron microscopy.

The aim of this work was to study the effect of the modification of titanium dioxide with silicon additives on the phase composition, microstructure, and pore structure of Ti–Si–O binary oxides in order to prepare new thermally stable nanomaterials based on TiO_2 (anatase).

EXPERIMENTAL

The titanium dioxide samples modified with silicon oxide additives in an amount of 1–15 wt % SiO_2 were prepared by the incipient wetness impregnation of anatase, which was prepared by the industrial sulfuric acid technology [30], with an alcoholic solution of tetraethyl orthosilicate followed by drying in air and then in a drying oven at 110°C for 12 h and thermal treatment in air over the temperature range of 400–1100°C for 4 h. Samples are designated as TS-wt % SiO_2-treatment temperature, °C.

The X-ray diffraction analysis of xerogels was performed on a URD-63 diffractometer with monochromated CuK_α radiation. The anatase crystallite size (D, nm) was estimated based on the size of coherent scattering regions (CSRs) from the Scherrer equation [31] using the halfwidths of 2.0.0 reflections (Table 1).

The electron-microscopic studies of the samples were performed on a JEM 2010 instrument with a resolution of 1.4 Å and an accelerating voltage of 200 kV.

The pore structure of the samples was studied using the low-temperature (77 K) sorption of nitrogen on a DigiSorb-2600 Micromeritics instrument. Table 2 summarizes the calculated texture parameters, where S_{BET} is the specific surface area calculated using the BET method, V_s is the limiting sorption space volume including the micro–meso pore volume, and D_{pore} is the predominant mesopore diameter. The surface area of meso- and macropores S_α (m^2/g) and the micropore volume V_μ (cm^3/g) were determined using a comparative method for the treatment of N_2 adsorption isotherms in accordance with a published procedure [32]. The mesopore size distribution was calculated from the desorption branch of an isotherm using the common Barret–Joyner–Halenda (BJH) method [33].

RESULTS AND DISCUSSION

The modification of titanium dioxide results in a considerable change in the temperature of the phase transition of anatase to rutile. X-ray diffraction techniques allowed us to state that, in modified samples with SiO_2 contents higher than 5 wt %, the rutile modification of titanium dioxide was almost not detected up to 1000°C, whereas it is well known that rutile was reliably detected in pure titanium dioxide even above 750°C (Table 1). At the minimum SiO_2 content (1 wt %), rutile became a predominant phase at 1000°C. As the calcination temperature was increased to 1100°C, rutile became the main crystalline phase in the samples with SiO_2 contents of less than 15 wt %, and the concentration of anatase remained as high as 80% at a SiO_2 content of 15 wt %. Note that the anatase crystallite size regularly decreased (at the same treatment temperatures) as the silicon dioxide content of the samples was increased.

The unit cell parameters (a and c) of anatase were insignificantly distorted in all cases; in the first approximation, they did not differ from the values for pure anatase prepared by the same method and unmodified [27].

However, a more precise consideration shows that both of the parameters a and c were somewhat smaller than standard values. Taking into account electron-microscopic data (see below), which are indicative of a defect structure of anatase particles in the samples

Table 1. Phase composition and structure characteristics of titanium dioxide and TiO_2–SiO_2 samples

Sample	Phase composition		Unit cell parameters		*D*, nm
	phase	concentration, wt %	*a*, Å	*c*, Å	
TiO_2-500	Anatase	100	3.789(1)	9.511(2)	20
TiO_2-750	Anatase	20	3.787(1)	9.514(1)	43
	Rutile	80	4.589(2)	2.955(2)	95
TiO_2-900	Rutile	100	4.590(2)	2.955(2)	>100
TS-1-500	Anatase	100	3.781(2)	9.494(5)	30
TS-1-750	Anatase	100	3.781(2)	9.493(5)	30
TS-1-900	Anatase	100	3.779(2)	9.505(5)	43
TS-1-1000	Anatase	25	3.779(2)	9.507(5)	68
	Rutile	75	4.587(2)	2.948(2)	90
TS-5-500	Anatase	100	3.788(5)	9.46(1)	10
TS-5-750	Anatase	100	3.781(2)	9.490(5)	20
TS-5-1000	Anatase	99	3.779(2)	9.508(5)	43
	Rutile	1	–	–	–
TS-5-1100	Anatase	1	–	–	–
	Rutile	99	4.590(2)	2.955(2)	>100
TS-7-500	Anatase	100	3.784(5)	9.48(1)	10
TS-7-1000	Anatase	95	3.784(2)	9.514(5)	45
	Rutile	5	–	–	90
TS-7-1100	Anatase	15	3.782(2)	9.515(5)	75
	Rutile	85	4.587(2)	2.956(2)	>100
TS-15-400	Anatase	100	3.785(5)	9.47(1)	10
TS-15-500	Anatase	100	3.784(5)	9.48(1)	10
TS-15-750	Anatase	100	3.779(2)	9.503(5)	18
TS-15-900	Anatase	100	3.779(2)	9.508(5)	23
TS-15-1000	Anatase	95	3.778(2)	9.502(5)	37
	Rutile	5	–	–	>100
TS-15-1100	Anatase	80	3.782(1)	9.519(4)	60
	Rutile	20	4.589(3)	2.957(3)	>100

calcined at a temperature lower than 1000°C, we can hypothesize with caution that silicon ions in a small (trace) amount can be stabilized in the anatase lattice. The silicon ions can be localized either at structural defects or at the sites of substitution for Ti^{4+} ions because the ionic radius of Si^{4+} (0.39 Å) is much smaller than the ionic radius of Ti^{4+} (0.64 Å) [34].

In the anatase structure, the chains of TiO_6 octahedra linked by shared vertices are arranged in (001) planes along the [100] and [010] directions. The octahedra of two parallel planes have common edges, and the faces of these octahedra form tetrahedrons (vacant in an ideal anatase structure) with A–O distances of 1.94 Å, where A is the center of the tetrahedron. It is obvious that the appearance of a silicon atom in a tetrahedrally coordinated position results in a considerable decrease in the size of the tetrahedron and the contraction of TiO_6 octahedra belonging to two different chains. As a consequence, the average Ti–O and O–O interatomic distances in the anatase structure and the unit cell parameter *c* decrease because the chains of TiO_6 octahedra belong to two parallel (001) planes.

Electron-microscopic data (Fig. 1) suggest that titanium dioxide modified with silicon oxide consists of bulky aggregates of particles of size to 1500 nm,

which are loosely packed. Figure 2 shows a high-resolution electron micrograph of sample TS-5-500. It can be seen that the sample is a nanostructured system consisting of coalesced anatase particles (7–10 nm) with wide amorphous layers of SiO_2 of size 0.3–1 nm in spaces between them. Microanalysis data suggest the presence of silicon in this sample, and the elemental composition of the sample (Si, 7.1 at %; Ti, 92.9 at %) is close to its chemical composition. An increase in the temperature to 750°C facilitates the growth of the anatase crystallite size to 10–15 nm with the retention of their nanocrystal structure (Fig. 3). The formation of closely packed TiO_2 aggregates, between which the layers of an amorphous silicon oxide phase are retained, can also be seen in Fig. 3.

From Fig. 4, it follows that, as the SiO_2 content of the sample was decreased to 15 wt %, the layer thickness of amorphous SiO_2 considerably increased to 2–5 nm and became comparable with the size of anatase crystallites (3–9 nm), which is consistent with the size D_{CSR} of anatase. Moreover, it can be seen that, in some regions of the sample structure, SiO_2 partially occurred on the surface of anatase particles.

The increase in the thermal treatment temperature of sample TS-15 to 1000°C was accompanied by further agglomeration of anatase particles; their size increased to 40 nm, which is also consistent with the size D_{CSR} of anatase. In this case, the structure of TiO_2 became regular, and SiO_2 as islands about 3–5 nm in size almost uniformly coated the anatase particle (Fig. 5).

Note that, from the electron micrographs of the samples calcined at 500–900°C, it follows that the formed anatase crystals were characterized by a defect structure, which manifested itself in irregular interplanar spacings. However, the structure of anatase crystallites became almost regular after calcination at 1000°C.

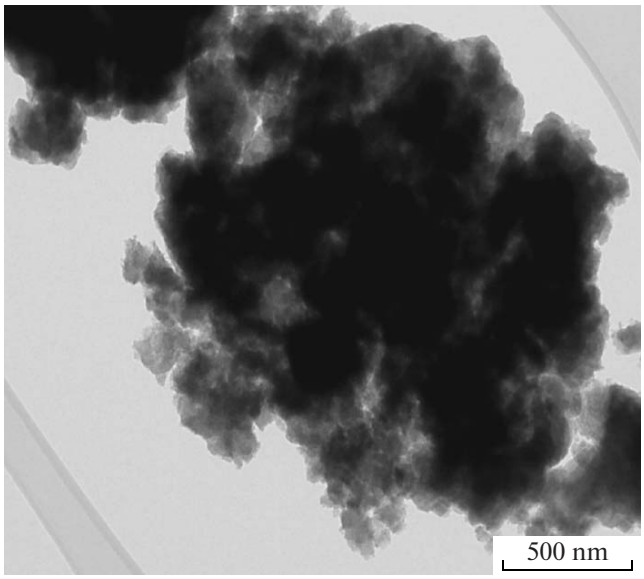

Fig. 1. Electron micrograph of sample TS-5-500.

Table 2. Pore structure parameters of titanium dioxide and TiO_2–SiO_2 samples

Sample	S_{BET}, m^2/g	V_s (V_μ), cm^3/g	D_{pore}, nm
TiO_2-500	92	0.316	7.4
TiO_2-750	13	–	–
TiO_2-900	2	–	–
TS-1-400	191	0.250	3.1
TS-1-500	111	0.285	6.0
TS-1-750	52	0,230	11.5
TS-1-900	23	0.126	9.2
TS-5-400	207	0.221	2.6
TS-5-500	130	0.239	3.9
TS-5-750	75	0.246	7.3
TS-5-900	52	0.174	5.9
TS-5-1000	12	0.075	–
TS-15-400	157	0.150 (0.023)	2.1
TS-15-500	137	0.151	2.6
TS-15-750	84	0.173	3.9
TS-15-900	53	0.108	3.8
TS-15-1000	11	0.079	–

The texture parameters of modified samples also exhibited special features. From Table 2, it follows that the specific surface areas of xerogels decreased with calcination temperature; however, this decrease was much smaller that in pure titanium dioxide. In this case, an increase in the concentration of silicon oxide resulted in the formation and retention of a larger surface area over the almost entire range of temperatures. The exception is sample TS-15-400; however, this is the sole sample in a series containing a noticeable micropore volume (V_μ = 0.023 cm^3/g). Because of

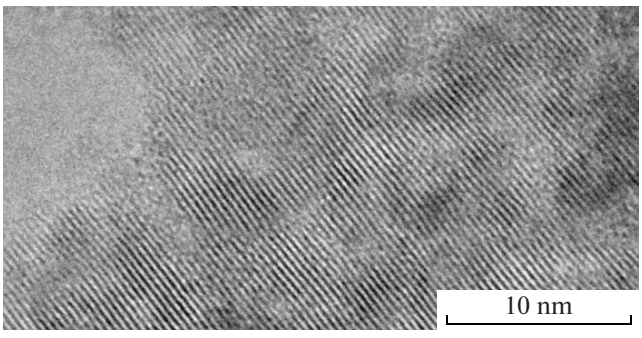

Fig. 2. High-resolution electron micrograph of sample TS-5-500.

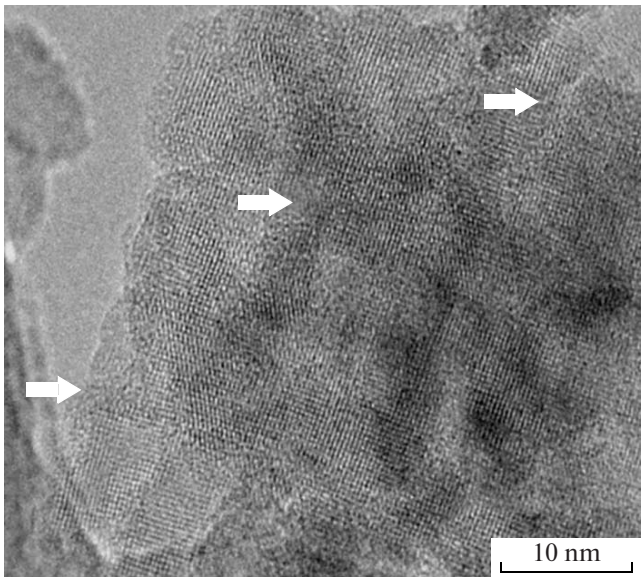

Fig. 3. Electron micrograph of TS-5-750 (arrows indicate silicon oxide layers).

this, the surface area calculated by the BET method is incorrect; moreover, the character of the pore structure is different from that of the samples calcined at a higher temperature. Note the following very important circumstance: samples TS-5 and TS-15 retained a highly developed specific surface area up to treatment temperatures of 900–1000°C.

The pore volume (V_s) of samples TS-5 and TS-15 remained almost unchanged in the course of thermal treatment up to 750°C and then began to decrease, whereas the decrease in the pore volume of sample TS-1 came into play at 500°C. In addition, the experimental data suggest that an increase in the silicon dioxide content of the samples caused a decrease in the pore volumes at calcination temperatures lower than 500°C.

Figures 6–10 show differential mesopore size distribution curves calculated using the BJH method. In Figs. 6 and 7, it can be seen that, as a rule, an increase in the thermal treatment temperature up to 900°C at a constant composition of xerogels was accompanied by an increase in the predominant pore size D_{pore} (see Table 2). At the same time, the calcination of samples at 1000°C resulted in the almost complete disappearance of the mesoporous part of the pore space and, correspondingly, in the impossibility of recognizing the predominant size of these pores.

Figures 8–10 show the effect of the composition of xerogels on the pore structure upon thermal treatment. From these data, it is clear that an increase in the concentration of silicon dioxide resulted in the formation of fine-pore samples, and this feature of the texture genesis was retained up to a thermal treatment at 900°C.

Considering the entire set of experimental data, we can state that the formation of the nanocrystalline structure of TiO_2 was formed upon the modification of titanium dioxide with silicon oxide using the procedure developed. This nanocrystalline structure of TiO_2 was formed by highly dispersed anatase particles of size 6–10 nm stabilized by silicon oxide layers formed by the decomposition of tetraethyl orthosilicate. An increase in the modifier concentration resulted in an increase in the thickness of the SiO_2 layer between anatase crystallites to inhibit the growth of anatase particles as a result of high-temperature agglomeration. According to Gribb and Banfield [19], this increased the phase transition temperature. Indeed, in the samples containing 5–15 wt % SiO_2, the anatase phase was stable up to 1000°C. In this case, as the con-

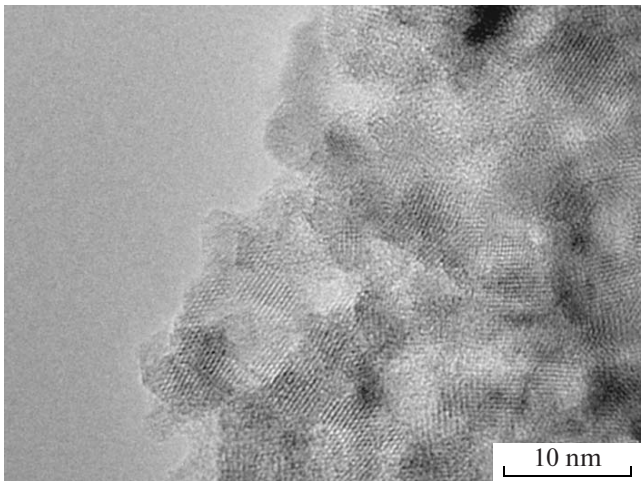

Fig. 4. High-resolution electron micrograph of TS-15-400.

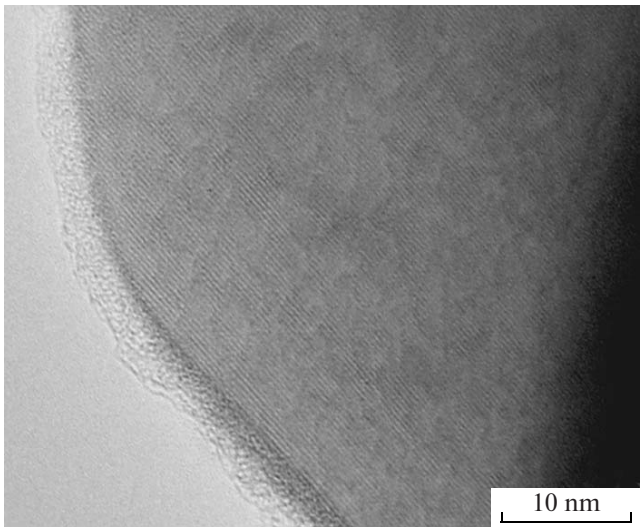

Fig. 5. High-resolution electron micrograph of TS-15-1000.

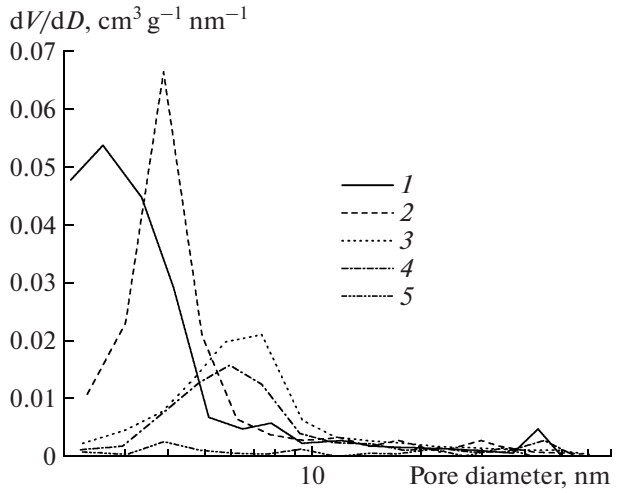

Fig. 6. Differential pore size distribution curves for TS-5 calcined at (*1*) 400, (*2*) 500, (*3*) 750, (*4*) 900, and (*5*) 1000°C.

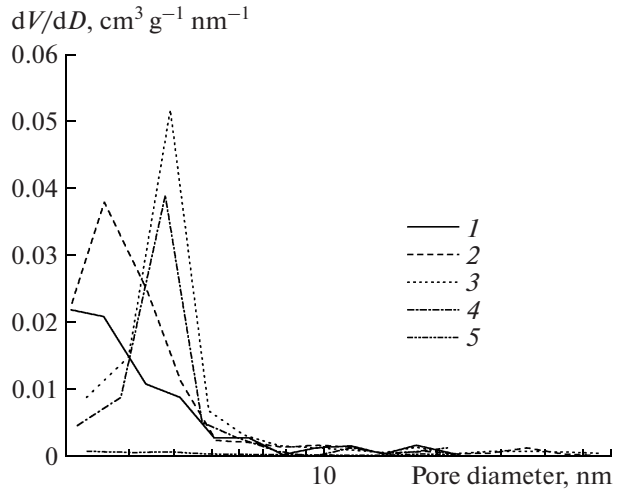

Fig. 7. Differential pore size distribution curves for TS-15 calcined at (*1*) 400, (*2*) 500, (*3*) 750, (*4*) 900, and (*5*) 1000°C.

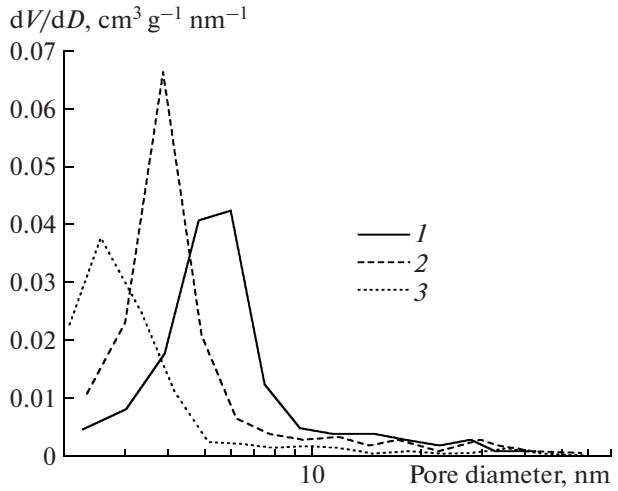

Fig. 8. Differential pore size distribution curves for (*1*) TS-1, (*2*) TS-5, and (*3*) TS-15 calcined at 500°C.

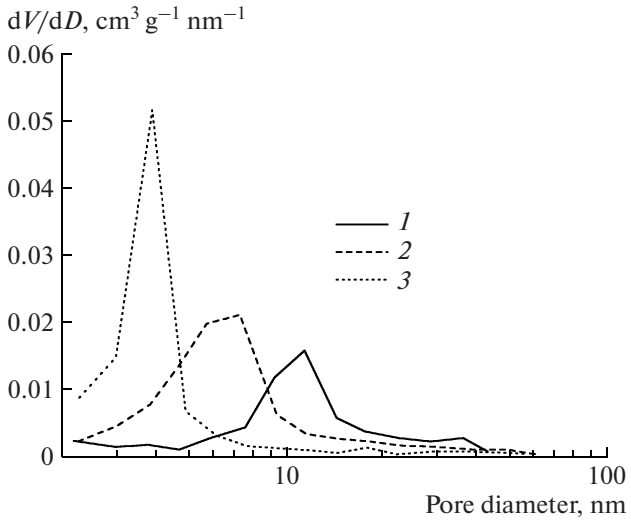

Fig. 9. Differential pore size distribution curves for (*1*) TS-1, (*2*) TS-5, and (*3*) TS-15 calcined at 750°C.

centration of SiO_2 was decreased, the temperature of the phase transition of anatase to rutile increased to a lesser extent. This may be explained by the fact that the amount of the modifier was insufficient for excluding contacts between anatase particles; as a result, they underwent agglomeration and conversion into rutile as a certain size was reached. At the same time, the stabilization of small amounts of silicon ions (at a trace impurity level) in the anatase structure cannot be completely excluded. In turn, this factor can also affect the temperature of the phase transition of anatase to rutile.

The formation of the pore structure of the binary system also depends on the effect of the increase in the phase transition temperature depending on the composition of the xerogel. It is believed that the formation of a noticeable micropore volume in sample TS-15-400 (Table 2) is related to the formation of bulky layers of amorphous SiO_2 (Fig. 4), where molecular-size pores with an enhanced adsorption potential are arranged. As the treatment temperature is increased, the layer thickness decreases and the structure regions with micropore properties disappear. Note that, evidently, the decrease in the total pore volume of samples with an increasing amount of introduced silicon dioxide and at a calcination temperature lower than 500°C is due to a decrease in the free space in the matrix of TiO_2 as a result of the arrangement of the modifier in these pores. The thermal stability of the

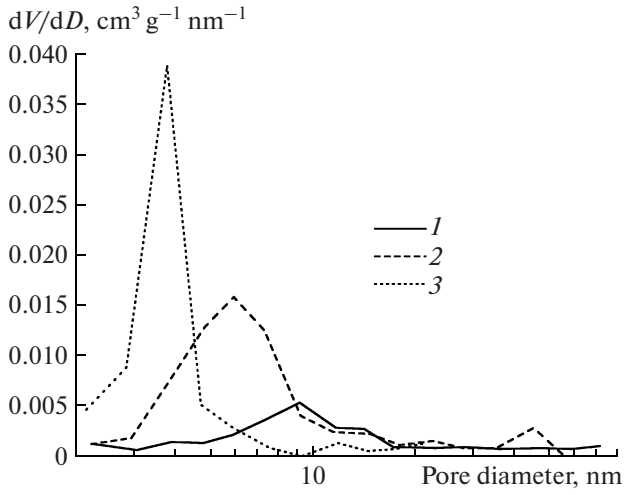

Fig. 10. Differential pore size distribution curves for samples (*1*) TS-1, (*2*) TS-5, and (*3*) TS-15 calcined at 900°C.

formed binary structure is supported by constant pore volumes for samples containing 5–15 wt % SiO_2 up to a treatment temperature of 750°C. The samples with lower modifier contents decrease their pore volumes even at a temperature higher than 500°C; this is also due to the insufficient thickness of the stabilizing layer of SiO_2.

It is believed that the above-mentioned interesting experimental fact of the formation of the fine-pore texture of the binary system (at the same treatment temperature) with increasing the introduced amount of the modifier is due to the retention of more dispersed anatase particles at a higher SiO_2 content. In this case, the pore space of mesopores is formed by the packing of smaller anatase particles and, correspondingly, characterized by a smaller predominant pore size (D_{pore}). The very fine pore texture with $D_{pore} \approx 4$ nm persists up to 900°C.

Thus, the modification of nanocrystalline titanium dioxide with an amorphous phase of silicon dioxide in accordance with the developed synthesis procedure allowed us to considerably increase the temperature of the phase transition of anatase to rutile and to form the thermally stable fine-pore texture of the TiO_2–SiO_2 binary system.

ACKNOWLEDGMENTS

We are grateful to A.V. Ishchenko for performing electron-microscopic studies.

REFERENCES

1. *Photocatalysis: Fundamentals and Applications*, Serpone, N. and Pelizzetti, E., Eds., New York: Wiley, 1989.
2. Kryukova, G.N., Zenkovets, G.A., Shutilov, A.A., Wilde, M., Gunter, K., Fassler, D., and Richter, K., *Appl. Catal., B*, 2007, vol. 71, no. 3, p. 169.
3. Vedrine, J.C., *Catal. Today*, 1994, vol. 20, no. 1, p. 171.
4. Alexeev, O.S., Chin, S.Y., Engelhard, M.H., Ortiz-Soto, L., and Amiridis, M.D., *J. Phys. Chem. B*, 2005, vol. 109, no. 49, p. 23430.
5. Park, N.-G., van de Lagemaat, J., and Frank, A.J., *J. Phys. Chem. B*, 2000, vol. 104, no. 38, p. 8989.
6. Kavan, L., Gratzel, M., Rathousky, J., and Zukal, A., *J. Electrochem. Soc.*, 1996, vol. 143, no. 2, p. 394.
7. Oliveri, G., Ramis, G., Busca, G., and Escribano, S.V., *J. Mater. Chem.*, 1993, vol. 12, no. 3, p. 1239.
8. Vejux, A. and Courtine, P., *J. Solid State Chem.*, 1978, vol. 23, nos. 1–2, p. 93.
9. Riyas, S., Krishnan, G., and Mohan Das, P.N., *Ceram. Int.*, 2006, vol. 32, no. 5, p. 593.
10. Strelko, V.V., Khainakov, S.A., Kvashchenko, A.L., Belyakov, V.M., and Bargun, A.I., *Zh. Prikl. Khim.*, 1988, vol. 61, no. 12, p. 3124.
11. Bondar', I.A., Glushkova, V.B., and Pozharskii, G.B., in *Vysokotemperaturnaya khimiya silikatov i okislov* (High-Temperature Chemistry of Silicates and Oxides), Leningrad: Nauka, 1972, p. 163.
12. Kleshchev, G.V., Sheinkman, A.I., and Bogirenko, Yu.A., *Lakokras. Mater.*, 1964, vol. 2, no. 11, p. 2143.
13. Zenkovets, G.A., Shutilov, A.A., Gavrilov, V.Yu., Tsybulya, S.V., and Kryukova, G.N., *Kinet. Katal.*, 2007, vol. 48, no. 5, p. 792 [*Kinet. Catal.* (Engl. Transl.), vol. 48, no. 5, p. 742].
14. Yuanzhi Li. and Sun-Jae Kim, *J. Phys. Chem. C*, 2005, vol. 109, no. 18, p. 6621.
15. Sasaki, T., Komatsu, Yu., and Fujiki, Y., *Solvent Extr. Ion Exch.*, 1983, vol. 1, p. 775.
16. Sasaki, T., Komatsu, Yu., and Fujiki, Y., *Sep. Sci. Technol.*, 1983, vol. 18, no. 1, p. 49.
17. Bondar', I.A., Glushkova, V.V., Tseitlin, P.A., Pozharskii, B.G., Derbeneva, T.F., and Sazonova, L.V., *Izv. Akad. Nauk SSSR, Neorg. Mater.*, 1971, vol. 7, no. 9, p. 1183.
18. Sheinkman, A.I., Gol'dshtein, L.M., Turlakov, V.N., and Kleshchev, G.V, *Zh. Prikl. Khim.*, 1972, vol. 45, nos. 4–6, p. 940.
19. Gribb, A.A. and Banfield, J.F., *Am. Mineral.*, 1997, vol. 82, nos. 7–8, p. 717.
20. Zhang, H. and Banfield, J.F., *J. Mater. Chem.*, 1998, vol. 8, no. 9, p. 2073.
21. Zhang, H. and Banfield, J.F., *J. Phys. Chem. B*, 2000, vol. 104, no. 15, p. 3481.
22. Orendorz, A., Brodyanski, A., Losch, J., Bai, L.H., Chen, Z.H., Le, Y.K., Ziegler, C., and Gnaser, H., *Surf. Sci.*, 2006, vol. 600, no. 18, p. 4347.
23. Zhang, H., Finnegan, M., and Banfield, J.F., *Nano Lett.*, 2001, vol. 1, no. 2, p. 81.
24. Zhang, H. and Banfield, J.F., *J. Phys. Chem. C*, 2007, vol. 111, no. 18, p. 6621.
25. Fu, Y., Gao, W., Xia, T., Zhou, L., and Tian, Y., *Gongneng Cailiao*, 2005, vol. 36, no. 2, p. 250.

26. Kholmanov, I.N., Barborini, E., Vinati, S., Piseri, P., Podesta, A., Ducati, C., Lenardi, C., and Milani, P., *Nunotechnology*, 2003, vol. 14, no. 11, p. 1168.
27. Zenkovets, G.A., Tsybulya, S.V., Burgina, E.B., and Kryukova, G.N., *Kinet. Katal.*, 1999, vol. 40, no. 4, p. 623 [*Kinet. Catal.* (Engl. Transl.), vol. 40, no. 4, p. 562].
28. Gao, X. and Wachs, I.E., *Catal. Today*, 1993, vol. 51, no. 2, p. 233.
29. Tuel, A., *Catal. Lett.*, 1998, vol. 51, nos. 1–2, p. 59.
30. Dobrovol'skii, I.P., *Khimiya i tekhnologiya oksidnykh soedinenii titana* (Chemistry and Technology of Oxide Compounds of Titanium), Sverdlovsk: Ural. Otd. Akad. Nauk SSSR, 1988.
31. Guinier, A., *Theorie et technique de la radiocristallographie*, Paris: Dunod, 1964.
32. Karnaukhov, A.P., *Adsorbtsiya. Tekstura dispersnykh i poristykh materialov* (Adsorption: Texture of Disperse and Porous Materials), Novosibirsk: Nauka, 1999.
33. Barret, E.P., Joyner, L.G., and Hallenda, P.H., *J. Am. Chem. Soc.*, 1951, vol. 73, no. 1, p. 373.
34. *Kataliticheskie svoistva veshchestv. Spravochnik* (Catalytic Properties of Substances: A Handbook), Roiter, V.A., Ed., Kiev: Nauk. Dumka, 1968.